Int J Adv Manuf Technol (2010) 48:495–503
DOI 10.1007/s00170-009-2321-3

ORIGINAL ARTICLE

A precision grinding method for screw rotors using CBN grinding wheel

Jing Wei · Guanghui Zhang

Received: 20 May 2009 / Accepted: 15 September 2009 / Published online: 1 October 2009

Abstract Aiming at the high precision machining of screw rotors, a new grinding method for screw rotors using cubic boron nitride (CBN) grinding wheel is presented in this paper. Small electroplated CBN grinding wheel is firstly used to grind screw rotors. The mathematical model for the axial profiles of CBN grinding wheel is developed based on gear engagement theory. Taking the backlash of screw rotors and the coating thickness of CBN layer into consideration, the modification of the base body of the wheel shape is introduced into the design of the CBN grinding wheel. Wire cut electrical discharge machining low speed (WEDM-LS) was used to machine the base body of the CBN grinding wheel. The formed turning tools of the base body of CBN grinding wheel using WEDM-LS and the wheel shapes of CBN grinding wheel using the formed turning tool were performed. The CBN grinding wheels for the screw rotors were made to verify the validity and effectiveness of the presented method. The electroplated CBN grinding wheels were used to machine the screw rotors, and the machining experiments were performed. The data obtained in the experiments reach the fifth class of Chinese Standard GB10095-88.

Keywords CBN grinding wheel · Precision grinding · Screw rotors · Modified wheel shape

J. Wei (✉)
School of Mechanical Engineering,
Dalian University of Technology,
Dalian 116-024, China
e-mail: weijing@dlut.edu.cn

G. Zhang
The State Key Lab.on Mechanical Transmissions,
Chongqing University,
Chongqing 400-030, China

Nomenclature

p	Screw parameter of rotor
H	Lead length of screw rotor
Σ	Mounting angle of the axes of grinding wheel and rotor
A_u	Distance between axes of grinding wheel and rotor
φ	Rotated angle as one point in screw rotor being contact point
x_1, y_1, z_1	Components at rotor profile in system σ_1
x, y, z	Components at rotor profile in system σ
x_u, y_u, z_u	Components at grinding wheel surface
n_x, n_y, n_z	General expression for normal vector of axis x, y, z components
n_u, n_u, n_u	General expression for normal vector of axis x_u, y_u, z_u components
$\vec{\omega}_u$	Angular velocity vector of grinding wheel
ω_{u}	Module of angular velocity $\vec{\omega}_u$
$\vec{\omega}_1$	Angular velocity of screw rotor
ω_1	Module of angular velocity ω_1
$\vec{v}_1$	Velocity of the contact point at rotor surface
$\vec{v}_1^0$	Initial velocity of the contact point at rotor surface
$\vec{v}_u$	Velocity of the contact point at wheel surface
$\vec{v}_u^0$	Initial velocity of the contact point at wheel surface
R_u	Theoretical radius of grinding wheel
Z_u	Theoretical axis position of grinding wheel
$R_u^{'}$	Modified radius of wheel surface
$Z_u^{'}$	Modified axis position of wheel surface
$\vec{n}_u$	Normal vector at wheel surface

1 Introduction

Screw rotors are the key part in screw compressors, screw kneaders, as well as screw pumps. The machining precision of the rotors determines the performance of machinery in large scales. Generally, milling cutters are used to machine the screw rotors. Many researchers, such as Xiao et al. [1] and Yao et al. [2], have done a lot of work on machining the screw rotors using milling cutters. This method can improve machining efficiency greatly. However, the low machining precision and surface accuracy are the main shortcomings. With increasing demands for high-performance technology, some new machining technologies have been developed to machine the screw rotors. British Holroyd industry [3] proposed a shaping grinding method in 1997 and provided a new system for the shaping grinding of precision spur, helical, worm gears, and screw compressor rotors. Katsumi et al. [4] used a built-up hob to machine screw compressor rotor. There are some other new methods introduced to machine screw rotors [5, 6].

As an effective precision grinding method, cubic boron nitride (CBN) grinding wheels have been widely used in industries for the past few decades, and they often produced very good results. Caglar and Evans [7] and Upadhyaya et al. [8] as well as Pavel and Srivastava [9] analyzed the advantages of this technique as follows: (1) CBN grinding wheels have high accuracy, consistency, and high wear resistance, and wheel dressing is unnecessary during the whole grinding process. (2) It has high accuracy profile for a ground workpiece. (3) It has excellent grinding performance and effectively avoids tooth surface burned or cracked. (4) It has high productivity, and the structure of grinding machine is quite simple. For CBN grinding wheels, there is no necessity for wheel dressing and wear compensation during the whole grinding. According to the reviews by a state of high-performance grinding, increased wheel speed can be achieved by highly efficient abrasives [10]. Most of the researches [11, 12] on the application of the CBN shape grinding focus on the material properties. In order to avoid thermal damage of the workpiece and to exploit the potential of CBN, Tonshoff et al. [13] developed a temperature model to predict residual stresses on the workpiece surface based on the grinding parameters. Jackson et al. [14] studied the basic mechanisms and the applications for the technology of high-speed grinding with CBN grinding wheels. They proposed developments in process technology associated with high-speed machining, and grinding machine and grinding tool also need to adapt to high-speed machining as well as to workpiece-related factors that influence machining results. Ding et al. [15] developed a new technology using monolayer brazed CBN grinding tools to machine difficult-to-cut materials. Based on gear engagement theory, You et al. [16] developed a mathematical model on calculating the profiles of CBN grinding wheel for involute gears, and the modification of gear shape was introduced into the design of CBN grinding wheel.

With increasing demands for high-speed and high-precision machining technology, a new grinding method for screw rotors using CBN grinding wheels is presented in this paper. Small electroplated CBN grinding wheel are firstly used to grind screw rotors. In grinding process, the precision of grinding wheel directly determines the ground workpiece precision. The correct and accurate profile of the wheel base body is a prerequisite for electroplating CBN grinding wheel. Aiming at the precision machining of CBN grinding wheel, a mathematical model on how to design the axial profiles of the CBN grinding wheel for machining screw rotors is developed based on gear engagement theory.

2 Shape design of CBN grinding wheel

2.1 The tooth surface equation of CBN wheel shape

Based on gear engagement theory, Litvin and Fuentes [17] established the coordinate systems of cylindrical worms machining and reported the contact equation of the grinding wheel and worm surface. Similarly, the helical surface of screw rotors can be regarded as the one to generate relative movement of a grinding wheel and a helical workpiece.

The coordinate systems are defined as follows: A fixed coordinate system σ is located in the center of the end section of the screw rotor. A coordinate system σ_u is fixed at the center of the grinding wheel. A moving coordinate system σ_1 is fixed at the rotor blank. The grinding wheel is considered to be at rest in the process of generation, and the rotor being generated performs screw motion around its axis with screw parameter p, where $p=H/2\pi$; the axes of the grinding wheel and the rotor are crossed, forming the mounting angle Σ. A_u is the distance between the axes of the screw rotor and the grinding wheel. Figure 1 shows the geometry relationship between a grinding wheel and a screw rotor.

During the process of grinding, a grinding wheel performs rotation around its axis, but this is related to the velocity of grinding only and can be ignored when the mathematical aspects of rotor generation are considered. The radii of a contact point M in coordinate systems σ_1 and σ_u are $\vec{r}$, $\vec{r}_u$, respectively. The transformations between σ and σ_u and σ and σ_1 can be expressed as Eqs. 1 and 2, respectively [17]. Figure 2 shows the kinematic relationships between a grinding wheel and a screw rotor.

$$\begin{pmatrix} x \\ y \\ z \\ 1 \end{pmatrix} = \begin{pmatrix} 1 & 0 & 0 & A_u \\ 0 & \cos\Sigma & -\sin\Sigma & 0 \\ 0 & \sin\Sigma & \cos\Sigma & 0 \\ 0 & 0 & 0 & 1 \end{pmatrix} \begin{pmatrix} x_u \\ y_u \\ z_u \\ 1 \end{pmatrix} \tag{1}$$

$$\begin{pmatrix} x \\ y \\ z \\ 1 \end{pmatrix} = \begin{pmatrix} \cos\varphi & -\sin\varphi & 0 & 0 \\ \sin\varphi & \cos\varphi & 0 & 0 \\ 0 & 0 & 1 & p\varphi \\ 0 & 0 & 0 & 1 \end{pmatrix} \begin{pmatrix} x_1 \\ y_1 \\ z_1 \\ 1 \end{pmatrix}. \tag{2}$$

2.2 Theoretical axial section of CBN grinding wheel

CBN grinding wheel is a revolution surface. Therefore, the geometry of CBN grinding wheel will be known if the axial section of the revolution surface is given. According to Figs. 1 and 2, the radii of a contact point M in coordinate systems σ_1 and σ_u can be expressed as Eq. 3:

$$\begin{cases} \vec{r}_1 = x_1\vec{i}_1 + y_1\vec{j}_1 + z_1\vec{k}_1 \\ \vec{r}_u = x_u\vec{i}_u + y_u\vec{j}_u + z_u\vec{k}_u. \end{cases} \tag{3}$$

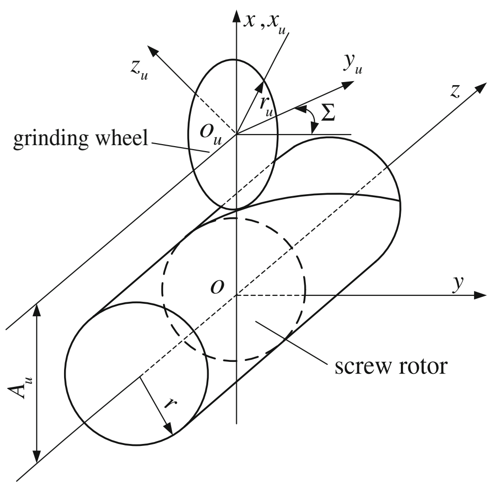

(a) Coordinate setting of the grinding wheel

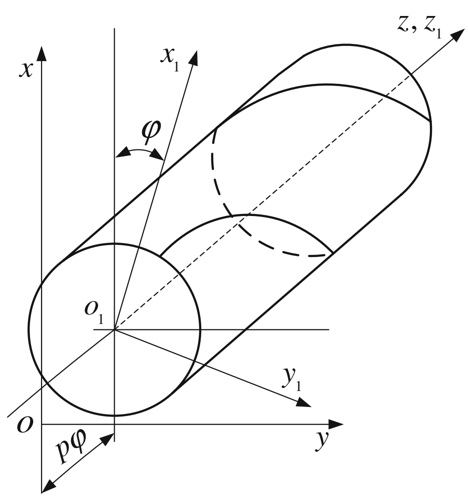

(b) Coordinate setting of the screw rotor

Fig. 1 Geometry relationship between a grinding wheel and a screw rotor

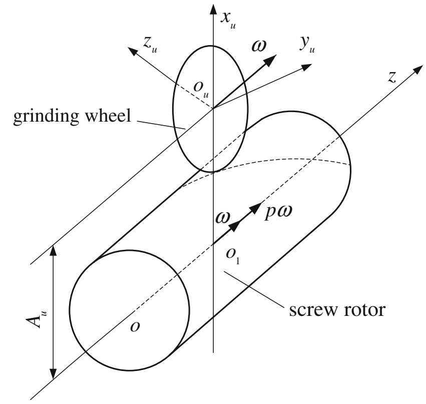

(a) Vectors in screw rotor and grinding wheel

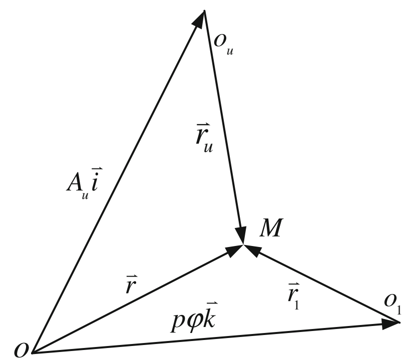

(b) Relationship of different vectors

Fig. 2 Kinematic relationship between a grinding wheel and a screw rotor

Equation 1 can be transformed as seen in Fig. 2b:

$$\begin{cases} \vec{r}_1 = \vec{r} - p\varphi\vec{k} = x\vec{i} + y\vec{j} + (z - p\varphi)\vec{k} \\ \vec{r}_u = \vec{r} - A_u\vec{i} = (x - A_u)\vec{i} + y\vec{j} + z\vec{k}. \end{cases} \tag{4}$$

The angular and the velocity of the contact point M in σ_1 and σ_u can be deduced as follows, respectively:

$$\begin{cases} \vec{\omega}_1 = \omega_1\vec{k}_1 \\ \vec{v}_1 = \vec{\omega}_1 \times \vec{r}_1 + \vec{v}_1^0 = \omega_1(-y_1\vec{i}_1 + x_1\vec{j}_1 + p\vec{k}_1). \end{cases} \tag{5}$$

$$\begin{cases} \vec{\omega}_u = \omega_u\vec{k}_u \\ \vec{v}_u = \vec{\omega}_u \times \vec{r}_u + \vec{v}_u^0 = \vec{\omega}_u(-y_u\vec{i}_u + x_u\vec{j}_u). \end{cases} \tag{6}$$

Then transform Eqs. 5 and 6 into the fixed coordinate system σ:

$$\begin{cases} \vec{\omega}_1 = \omega_1\vec{k} \\ \vec{v}_1 = \omega_1(-y\vec{i} + x\vec{j} + p\vec{k}). \end{cases} \tag{7}$$

$$\begin{cases} \vec{\omega}_u = \omega_u(-\sin\Sigma\vec{j} + \cos\Sigma\vec{k}) \\ \vec{v}_u = \omega_u[(-z\sin\Sigma - y\cos\Sigma)\vec{i} \\ \qquad + (x - A_u)\cos\Sigma\vec{j} + (x - A_u)\sin\Sigma\vec{k}]. \end{cases} \tag{8}$$

Substitute $\vec{v}_1$ and $\vec{v}_u$ as $\vec{v}^{1u} = \vec{v}_1 - \vec{v}_u$; the relative speed $\vec{v}^{1u}$ of the contact point M can be given by Eq. 9:

$$\vec{v}^{1u} = \omega_1(-y\vec{i} + x\vec{j} + p\vec{k}) - \omega_u[(-z\sin\Sigma - y\cos\Sigma)\vec{i} + (x - A_u)\cos\Sigma\vec{j} + (x - A_u)\sin\Sigma\vec{k}]. \tag{9}$$

The contact point M should satisfy the equation $\vec{n} \times \vec{v}^{1u} = 0$. Substituting Eq. 9 and $\vec{n}$ into the equation $\vec{n} \times \vec{v}^{1u} = 0$, where $\vec{n}$ is the normal vector of the helical tooth profile as in Appendix, the contact equation can be expressed as:

$$\vec{n} \times \omega_1(-y\vec{i} + x\vec{j} + p\vec{k}) - \omega_u \times \vec{n} \times [(-z\sin\Sigma - y\cos\Sigma)\vec{i} + (x - A_u)\cos\Sigma\vec{j} + (x - A_u)\sin\Sigma\vec{k}] = 0. \tag{10}$$

Considering the properties of $\vec{n} \times \omega_1(-y\vec{i} + x\vec{j} + p\vec{k}) = 0$ and $n_x y - n_y x = p n_z$ of cylindrical helicoids, the contact equation Eq. 10 can be further modified as follows:

$$z n_x + A_u \cot\Sigma n_y + (A_u - x + p\cot\Sigma) n_z = 0. \tag{11}$$

Hence, the trajectory between a grinding wheel and a screw rotor can be deduced by the clustering tooth profile points of the helical surface, which satisfy Eq. 11. The theoretical axial section of the CBN grinding wheel can be given as Eq. 12:

$$\begin{cases} R_u = \sqrt{x_u^2 + y_u^2} \\ Z_u = z_u. \end{cases} \tag{12}$$

2.3 Modification of the theoretical axial section

Considering those inevitable factors, such as manufacture and assembly errors, deformations, thermal expansions, etc., the backlash, δ_b, of two rotors should be given. Furthermore, the coating thickness, δ_c, of CBN layer should be considered. Therefore, the design of the modified grinding wheel surface should take the backlash, δ_b, of two rotors and the coating thickness, δ_c, of CBN layer into account. The relationship between the modified value δ of the theoretical axial section of grinding wheel and the backlash, δ_b, as well as the coating thickness, δ_c, is given by:

$$\delta = \delta_b - \delta_c. \tag{13}$$

Actually, the modified profiles of the grinding wheel can be achieved by three steps. Firstly, obtain the theoretical axial section cc (expressed by a series of discrete points) of the wheel body of CBN grinding wheel calculated from Eq. 12. Secondly, obtain the normal vectors of the theoretical profiles of the grinding wheel. Thirdly, obtain the modified axial section $c'c'$ with surface equidistance method. The modified axial section of CBN grinding wheel satisfies Eq. 14:

$$\begin{cases} R_u' = R_u + \delta\sqrt{1 - \cos^2\varepsilon} \\ Z_u' = Z_u + \delta\cos\varepsilon. \end{cases} \tag{14}$$

The angle ε between normal vector $\vec{n}_u$ and rotation vector $\vec{k}_u$ of the grinding wheel can be obtained from Eq. 15:

$$\cos\varepsilon = \frac{\vec{k}_u \times \vec{n}_u}{|\vec{n}_u|}. \tag{15}$$

The direction of the normal vector $\vec{n}_u$ and the normal vector $\vec{n}$ in the trajectory between the grinding wheel and the screw rotors is identical. In coordinate system σ, $\vec{n}_u$ can be expressed as:

$$\vec{n}_u = n_x\vec{i} + n_y\vec{j} + n_z\vec{k}. \tag{16}$$

From the transformation between σ_u and σ:

$$\vec{k}_u = -\sin\Sigma\vec{j} + \cos\Sigma\vec{k}. \tag{17}$$

Substituting Eqs. 16 and 17 into Eq. 15, ε can be given by Eq. 18:

$$\cos\varepsilon = \frac{n_z\cos\Sigma - n_y\sin\Sigma}{\sqrt{n_x^2 + n_y^2 + n_z^2}}. \tag{18}$$

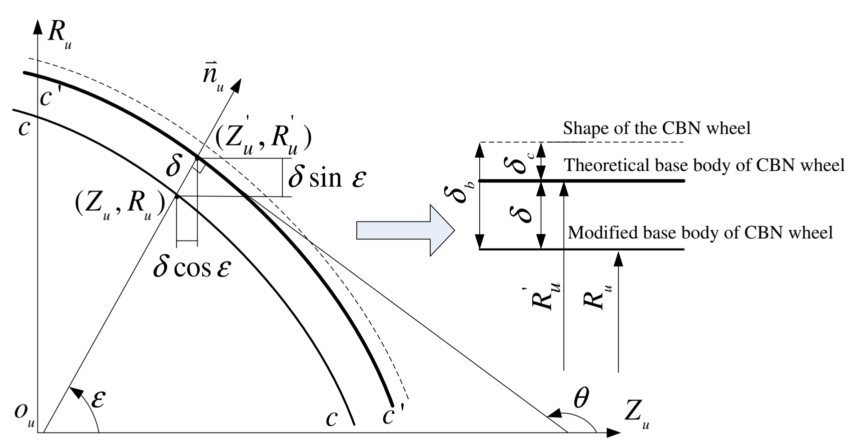

Fig. 3 Modified axial section with surface equidistance method

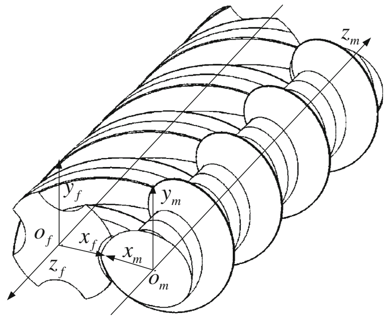

(a) 3D profiles of screw rotors

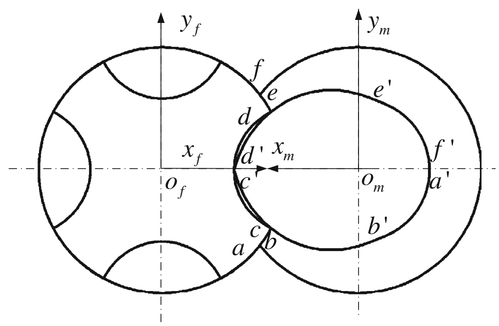

(b) End section of screw rotors

Fig. 4 Rotor profiles of one novel twin-screw kneader

Figure 3 shows the calculation of modified axial section with surface equidistance method. In Fig. 3, the tangent angle θ at each point at the theoretical axial section should satisfy the following:

If $0\leq\varepsilon\leq\pi/2$, the tangent angle θ at each point is an obtuse angle. Then the relationship between ε and tangent angle θ is given by $\theta=\pi/2+\varepsilon$; when $\pi/2<\varepsilon\leq\pi$, the tangent angle θ at each point is an acute angle; then the relationship between ε and tangent angle θ is given by $\theta=\pi-\varepsilon$.

The profiles of the modified wheel shape calculated using the above method can be expressed as a sequence of discrete set of points. In order to obtain numeric control (NC) code, these discrete set of points should be pretreated. The arc interpolation should be applied because the linear interpolation function will induce more interpolation segments which will generate a large quantity of NC codes and may lead to tremendous vibration of the machine tool; this in turn will reduce the machining precision of the CBN grinding wheel.

The arc interpolation segments can be obtained using the arc spline fitting method or the biarc spline method. Yang and Wang [18] faired and fitted planar point sets using minimal energy arc splines by computing the optimal tangents for curve interpolation and adjusting the point positions. Meek and Walton [19] approximated clothoid using arc splines. But the arc splines cannot preserve the first arc continuity because the tangents of two adjacent arcs at the connecting node are different. According to the reports [20], a biarc is composed of two consecutive circular arcs with an identical tangent at connecting node. Since the tangents at the connecting node are the same, the first arc continuity can be preserved. In addition, if the difference between the curvatures at the connecting node was minimized, the second arc smoothness can be enhanced. Besides geometry invariability, the biarc spline method seems to be easier and more accurate than other spline methods; especially, it can avoid solving the non-convergent and nonlinear equations. As an approximation criterion, the biarc segments are used to approximate the profile of grinding wheel based on allowed maximum deviation distance in this paper. These arcs generated by the biarc method can be post-processed for NC code generation on machining the base body of CBN grinding wheel.

3 Calculation and experiment

For one novel continuous twin-screw kneader reactor, the number of female rotor (right hand) and male rotor (left hand) teeth are four and one, respectively; both the outer diameters of the female rotor and the male rotor are 60 mm; the lead length of the rotors are 200 and 50 mm,

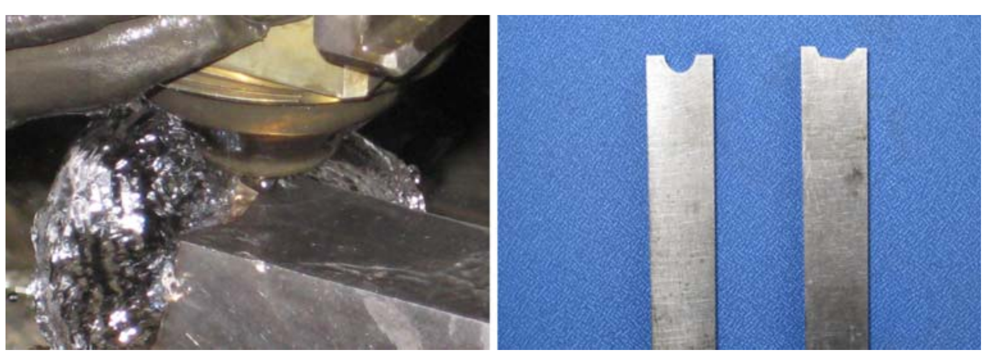

(a) Machining formed turning tool (b) Formed turning tool machined by WEDM-LS

Fig. 5 Machining-formed turning tool using WEDM-LS

Fig. 6 Machining wheel shapes of CBN grinding wheel using shaping bath tool

(a) Wheel base body for female screw rotor (b) Wheel base body for male screw rotor

respectively; the backlash between the female and male rotors is $\delta_b^{'} = 0.2$ mm. Figure 4 shows the end section of the female and male rotors in one novel twin-screw kneader reactor.

The high precision manufacturing of the base body of CBN grinding wheel is one of the key technologies using electroplated CBN grinding wheel. Forming turning can simplify the cutting motion further to improve the precision and efficiency of the CBN grinding wheel. In order to improve the precision, wire cut electrical discharge machining low speed (WEDM-LS) is used to machine the base body of the CBN wheel in this paper. The machining of the formed turning tool of the base body of the CBN wheel using WEDM-LS are shown in Fig. 5. In Fig. 5a, the formed turning tool for male rotor was machining by WEDM-LS. Figure 5b showed the finished formed turning tool machined by WEDM-LS. The left one is for the female rotor and the right one is for the male rotor mentioned above. The base bodies of CBN grinding wheel for female and male screw rotors being machined using formed turning tool are shown in Fig. 6a, b, respectively.

The base bodies of CBN wheel for female and male rotors were made of 45 steel in this paper. The grinding efficiency of CBN tool depends, to a greater extent, on the grit size of tools. The term "grit size" here means the sizes of CBN crystals. CBN abrasive material spec DLII, grit size no. 150#, was selected with the nominal particle size range of 75–106 μm. The average of grit size is δ_{c1}= 90.5 μm. Ni–Co–CBN composite plating on grinding wheel was prepared by conventional electro co-deposition method on the 45 steel. The production process of electroplating CBN grinding wheel is as below: cutting→ quenching and tempering treatment→turning→wheel base body→surface protection of wheel base body→electroplating CBN crystals on the wheel base body→CBN grinding wheel.

Given the CBN basement thickness δ_{c2}=0.05 mm and the backlash of δ_b=0.1 mm. Given different mounting distances A_u and angles Σ, different profiles of the CBN grinding wheel can be obtained. In this study, the mounting distance A_u and angle Σ for the female rotor are A_u= 150 mm and Σ=45°; the mounting distance A_u and the angle Σ for the male rotor are A_u=150 mm and Σ=−45°, respectively. The design parameters of the CBN wheel for the female and male rotors of twin-screw kneader are listed in Table 1.

Table 1 Design parameters of female and male rotors for twin-screw kneader

Parameters	Female rotor	Male rotor
Lead *H* (mm)	200	50
Teeth number	4	1
Screw direction	Right	Left
Lead angle in reference circle (°)	53°16′20″	18°31′27″
Axial modulus	15.9154	15.9154
Length *L* (mm)	400	400
Outer diameters of rotors D_r (mm)	60	60
Distance between female and male rotors *A* (mm)	47.5	47.5
Mounting distance A_u (mm)	150	150
Mounting angle Σ (°)	45	−45
Theoretical diameters of CBN wheel D_u (mm)	82.50	85.427

Fig. 7 CBN grinding wheel for machining the screw rotors

(a) Base body of CBN grinding wheel (b) CBN grinding wheel

A series of arcs were obtained according to the method as described in Sections 2 and 3. These arc segments were used as the NC code using biarc approximation method after the tangent value of each point was calculated. For all the arcs, if the radii of arc segments are positive, the arc interpolations should be in anticlockwise direction; otherwise, the arc interpolations should be in clockwise direction. Meanwhile, the radii of the arc interpolations should be calculated to check whether they were greater than the maximal radius of the interpolation of machine controller. Lines, instead of arcs, should be used in NC code generation directly if the radii were greater than the maximal radius. Then, the selected CBN materials were electroplated on the wheel base body. The finished base body of the CBN wheel and the finished CBN grinding wheel for machining the rotors of novel twin-screw kneader are shown in Fig. 7a, b, respectively. In Fig. 7a, b, the left finished base body of CBN wheel and left finished CBN wheel were for the female rotor and the right ones for the male rotor, respectively.

Grinding experiments were performed on a native vertical milling machine XKA5040A. The largest workpiece of the machine tool has dimension 320×1320 mm. One self-made high-speed grinder was connected with the main shaft of the milling machine. The main shaft of the grinder can reach 180 revolutions per second. The grinding speed on the outer surface of CBN wheel can reach 45–48 m/s. Chemical reactions will occur if CBN abrasive crystal encounters alkaline aqueous solution, which will result in CBN abrasive crystal damaged under high temperature in the grinding process; thus, oil-based coolant should be used. High-performance non-active cutting oil, Decoll 703, one kind of yellowish brown translucent liquid with movement viscosity of 10–13 m^2/s and flash point of 170°C, was used in experiment during ground. Grinding machining of the screw rotors using CBN grinding wheel is shown in Fig. 8. Figure 8a is the grinding of the female rotors and Fig. 8b the grinding of the male rotors. The two rotors machined by CBN grinding wheel are shown in Fig. 9.

The accuracy of the screw rotors was measured on the profile checking instrument ZC/668H CMM; the measuring strokes are 600×800×600 mm. The accuracy according to ISO10360-2 is maximum permissible indication error, 1.2 µm+L/1,000; maximum permissible probing error, 1.2 µm. For actual measurement results, the helix tolerance of female and male rotors is 17.5–21 µm; total composite tolerance of axial pitch is 8.5–13.5 µm; limit deviation of axial pitch is 65.5–72.5 µm; and profile error is 6.5–8 µm. Surface roughness is measured in a surface roughometer,

Fig. 8 Grinding machining of the screw rotors using CBN grinding wheel

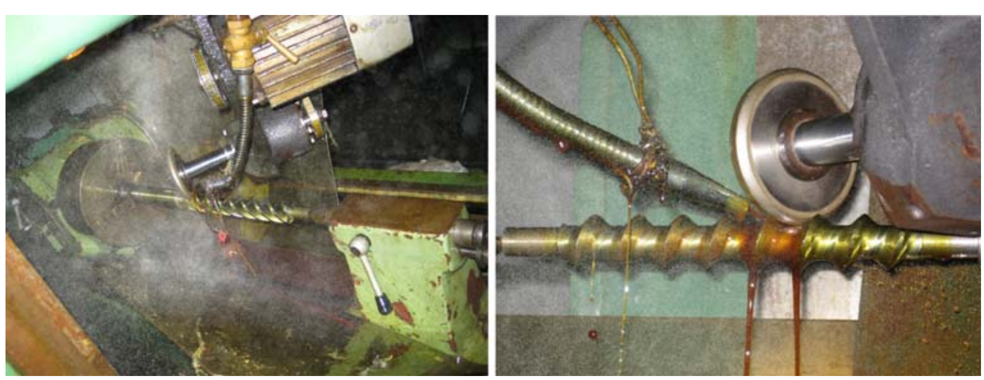

(a) Grinding machining of the male rotors (b) Grinding machining of the female rotors

Fig. 9 Screw rotors machined by CBN grinding wheel

SJ–401, which is made by Mitutoyo Company. The minimum and maximum values of the surface roughness measured in surface roughometer of the two rotors are 0.5 and 0.65 μm, respectively. The data obtained in the experiments reach the fifth class of the Chinese Standard GB10095-88 (essentially equivalent to ISO1328-1975). The measurement results are shown in Table 2.

4 Conclusions

In this study, small CBN grinding wheels were used to machine screw rotors. A mathematical model was proposed to calculate the theoretical axial section of the CBN grinding wheel based on gear engagement theory. Taking the backlash, δ_b, of rotors and the coating thickness, δ_c, of CBN layer into consideration, the theoretical axial section of CBN grinding wheel was modified with the surface equidistance method.

According to the method presented in this paper, the profiles of CBN grinding wheel can be calculated correctly and accurately. The experimental results show that it is feasible to grind screw rotors using electroplating CBN grinding wheel. Compared with traditional grinding wheel, the rigidity and efficiency of CBN grinding wheel has been improved greatly. CBN grinding wheel does not need to renovate; thereby, it cannot only increase economic efficiency but also save time and reduce cost. The method can meet the requirement of high-precision machining for screw rotors without any grinding burns and cracks and will have a broad application prospect in the future. The experimental results confirmed that the method presented here can be used in the precision machining of screw rotors using CBN grinding wheels. Actually, the method presented in this paper could be used to machine other cylindrical helicoids, such as column worms, helical gears, and spiral gears.

Acknowledgments This research was supported by National Natural Science Foundation of China (no. 50905023). The authors would like to take this opportunity to express their sincere appreciation.

Appendix: Normal vector on helical tooth profile of the screw rotors

Suppose the helical tooth profile can be expressed in rotor coordinate system σ_1 as:

$$\begin{cases} \vec{r}(u,v) = x_1(u,v)\vec{i}_1 + y_1(u,v)\vec{j}_1 + z_1(u,v)\vec{k}_1 \\ x_1(u,v) = x_0(u)\cos v - y_0(u)\sin v \\ y_1(u,v) = x_0(u)\sin(v) + y_0(u)\cos v \\ z_1(u,v) = pv. \end{cases} \tag{19}$$

where u and v are parameters of the helical tooth profile; p is the screw parameter of screw rotor; and $x_0(u)$, $y_0(u)$ are the components at the end section profile of helical rotor in coordinate system σ_1. The normal vector $\vec{n}$ on the helical tooth profile can be expressed as:

$$\vec{n} = \vec{r}_u \times \vec{r}_v = \begin{vmatrix} \vec{i}_1 & \vec{j}_1 & \vec{k}_1 \\ \vec{r}_{xu} & \vec{r}_{yu} & \vec{r}_{zu} \\ \vec{r}_{xv} & \vec{r}_{yv} & \vec{r}_{zv} \end{vmatrix}. \tag{20}$$

From the end section of screw rotor and the above equation, the normal vector $\vec{n}$ can be obtained as follows:

$$\begin{cases} \vec{n} = n_x\vec{i}_1 + n_y\vec{j}_1 + n_z\vec{k}_1 \\ n_x = p\left[x_0'(u)\sin v + y_0'(u)\cos v\right] \\ n_y = -p\left[x_0'(u)\cos v - y_0'(u)\sin v\right] \\ n_z = x_0(u)x_0'(u) + y_0(u)y_0'(u). \end{cases} \tag{21}$$

where $x_0'(u)$ is the first-order derivative of $x_0(u)$ and $y_0'(u)$ is the first-order derivative of $y_0(u)$.

Table 2 Accuracy of the rotors using CBN grinding wheel

	Female rotor	Male rotor
Helix tolerance (μm)	21.0	17.5
Total composite tolerance of axial pitch (μm)	13.5	8.5
Limit deviations of axial pitch (μm)	72.5	65.5
Profile error (μm)	8	6.5
Surface roughness (μm)	0.65	0.5

References

1. Xiao DZ, Li KB, Wang ZQ, Liu DM (1996) Computer aided design software package for conjugate helical surfaces. J Mater Process Technol 61:72–77
2. Yao LG, Ye ZH, Dai JS, Cai HY (2005) Geometric analysis and tooth profiling of a three-lobe helical rotor of the Roots blower. J Mater Process Technol 170:259–267
3. Couey JA, Marsh ER, Knapp BR, Vallance RR (2005) Monitoring force in precision cylindrical grinding. Precis Eng 29:307–314
4. Katsumi K, Kazumasa K, Hisashi T (2001) Gear-cutting tool for screw-compressor rotors (built-up hob). JSME Int J Ser C Mech Syst Mach Elem Manuf 44:802–807
5. Suh JD, Lee DG (2001) Manufacture of composite screw rotors for air compressors by RTM process. J Mater Process Technol 113:196–201
6. Stosic N (2006) A geometric approach to calculating tool wear in screw rotor machining. Int J Mach Tools Manuf 46:1961–1965
7. Caglar M, Evans R (2002) Grinding fluid performance and characterization of wheel wear in grinding using electroplated CBN Wheels. Abrasives Magazine. August/September, B-14
8. Upadhyaya RP, Fiecoat JH, Malkin S (2007) Factors affecting grinding performance with electroplated CBN wheels. CIRP Annals–Manufacturing Technology 56:339–342
9. Pavel R, Srivastava A (2007) An experimental investigation of temperatures during conventional and CBN grinding. Int J Adv Manuf Technol 33:412–418
10. Kopac J, Krajnik P (2006) High-performance grinding—a review. J Mater Process Technol 175:278–284
11. Inoue K, Sonoda H, Deng G, Yamanaka M, Kato M (1998) Effect of CBN grinding on the bending strength of carburized gears. J Mech Des 120:606–611
12. Sanchez Jose A, Ortega N, de Lacalle LNL, Lamikiz A, Marañon JA (2006) Analysis of the electro discharge dressing (EDD) process of large-grit size CBN grinding wheels. Int J Adv Manuf Technol 29:688–694
13. Tonshoff HK, Wobker HG, Brunner G (1995) CBN grinding with small wheels. Annals of the CIRP 44:311–316
14. Jackson MJ, Davis CJ, Hitchiner MP, Mills B (2001) High-speed grinding with CBN grinding wheels—applications and future technology. J Mater Process Technol 110:78–88
15. Ding WF, Xu JH, Shen M, Fu YC, Xiao B, Su HH, Xu HJ (2007) Development and performance of monolayer brazed CBN grinding tools. Int J Adv Manuf Technol 34:491–495
16. You HY, Ye PQ, Wang JS, Deng XY (2003) Design and application of CBN shape grinding wheel for gears. Int J Mach Tools Manuf 43:1269–1277
17. Litvin FL, Fuentes A (2004) Gear geometry and applied theory, 2nd edn. Cambridge University Press, UK, pp 565–569
18. Yang XN, Wang GZ (2001) Planar point set fairing and fitting by arc splines. Computer-Aided Des 33:35–43
19. Meek DS, Walton DJ (2004) An arc spline approximation to a clothoid. J Comput Appl Math 170:59–77
20. Tseng YJ, Chen YD (2000) Three dimensional biarc approximation of freeform surfaces for machining tool path generation. Int J Prod Res 38:739–763